GEOPHYSICS, VOL. 77, NO. 3 (MAY-JUNE 2012); P. WA99–WA107, 9 FIGS.
10.1190/GEO2011-0266.1

A microelectromechanical system digital 3C array seismic cone penetrometer

Ranajit Ghose[1]

ABSTRACT

A digital 3C array seismic cone penetrometer has been developed for multidisciplinary geophysical and geotechnical applications. Seven digital triaxial microelectromechanical system accelerometers are installed at 0.25-m intervals to make a 1.5-m-long downhole seismic array. The accelerometers have a flat response up to 2 kHz. The seismic array is attached to a class 1 digital seismic cone, which measures cone tip resistance, sleeve friction, pore-pressure, and inclination. The downhole 3C array can be used together with impulsive seismic sources and/or high-frequency vibrators that are suitable for high-resolution shallow applications. Results from two field experiments showed that a good data quality, including a constant source function within an array, and a dense depth-sampling allowed robust estimation of seismic velocity profiles in the shallow subsoil. Using horizontal and vertical seismic sources, downhole 9C seismic array data can be easily acquired. The quality of the shear-wave data is much superior when the surface seismic source is a controlled, high-frequency vibrator in stead of a traditional sledge hammer. A remarkable correlation in depth, in a fine scale, between low-strain seismic shear wave velocity and high-strain cone tip resistance could be observed. The array measurements of the full-elastic wavefield and the broad spectral bandwidth are useful in investigating frequency-dependent seismic wave propagation in the porous near-surface soil layers, which is informative of the in situ fluid-flow properties. Stable estimates of dispersive seismic velocity and attenuation can be obtained.

INTRODUCTION

The small strain ($<10^{-4} - 10^{-5}$) shear modulus estimated from the seismic shear-wave velocity V_S is an essential input for prediction of ground motion due to earthquake excitation, for evaluation of foundations for vibrating equipment and behavior of offshore structures during wave loading, and for deformation around excavations. Nearly three decades ago, seismic cone penetration testing (SCPT) was introduced as a rapid and economic means to obtain in situ V_S profiles in soil (Robertson, 1982; Campanella and Robertson, 1984; Campanella et al., 1986; Robertson et al., 1986). In cone penetration testing (CPT), essentially a steel rod with a cone-shaped tip is pushed into the ground while measurements are made with sensors located close to the tip. The cone is pushed using hydraulic rams. In SCPT, a geophone or an accelerometer is located in the cone. In addition to the usual cone tip resistance q_c and sleeve friction f_s, the shear wave generated at the surface is recorded at a regular depth interval by a propagating cone in the soil. Subsequent developments have resulted in improved accuracy and addition of sensors measuring pore pressure u, inclination I, temperature T, electrical resistivity R, etc., (see, e.g., Lunne et al. [1997] for a discussion).

Over the years, the use of SCPT has seen a steady growth. The minimally invasive nature and the possibility of simultaneous measurement of multiple parameters are attractive features. The continuous readings of the CPT provide fine details in the soil profile to define the layering and strata interfaces, as well as presence of clay seams, lenses, and sand stringers. The addition of V_S information through SCPT helps better discerning the atypical geomaterials, e.g., cemented and structured soils. The use of two seismic sensors, separated by 0.5 or 1 m, in the cone instead of one has become more common to get interval V_S (e.g., Sully and Campanella, 1995; Butcher and Powell, 1995). A frequent-interval V_S measurement method for improving the depth resolution is proposed by McGillivray (2007); in this approach, overlapping measurements in depth are made, but the source function is not the same between the

Manuscript received by the Editor 22 July 2011; revised manuscript received 3 January 2012; published online 23 April 2012.
[1]Delft University of Technology, Department of Geotechnology, Delft, The Netherlands. E-mail: r.ghose@tudelft.nl.
© 2012 Society of Exploration Geophysicists. All rights reserved.

Downloaded 27 Apr 2012 to 131.180.60.197. Redistribution subject to SEG license or copyright; see Terms of Use at http://segdl.org/

overlapping measurements. Downhole and crosshole geometries have been used in SCPT for assessing anisotropy in soil (e.g., Baldi et al., 1988; Sully and Campanella, 1995). Seismic waves generated by surface multioffset sources and recorded by 3C accelerometers in SCPT have been used for tomographic imaging of permafrost (LeBlanc et al., 2006).

Field-observed correlations in SCPT between q_c and V_S are used by many authors (e.g., Baldi et al., 1989; Mayne and Rix, 1993; Hegazy and Mayne, 1995; Eslaamizaad and Robertson, 1998; Simonini and Cola, 2000, Andrus et al., 2004; Schneider et al., 2004, among others). The V_S changes from SCPT are linked with the reflections seen in surface shear wave data to extend 1D information of soil stratigraphy to 2D or 3D (Ghose et al., 1996, 2002; Brouwer et al., 1997; Jarvis and Knight, 2000; Ghose and Goudswaard, 2004; Knight and Pidlisecky, 2005). The details of the transition at an interface as seen by CPT is extracted from the surface seismic reflections by exploiting the multiscale behavior of the local V_S field and q_c (Ghose and Goudswaard, 2004).

The usefulness of SCPT can greatly be improved and extended if the total (3C) seismic wavefield generated by fixed vertical and horizontal seismic sources at the surface and then modified due to propagation through the soil layers can be sampled densely and reliably at multiple depths (thus, the source effect remaining constant at all depths in an array) for a wide frequency range and if the influence of receiver coupling variations at different depths can be minimized. A common source gather recorded downhole will allow a good estimation of seismic velocity and attenuation. Array data processing techniques can be applied to such data sets. For subsoil investigation, it is advantageous to integrate multiple parameters (e.g., q_c, f_s, u, and V_S) that are measured in situ and simultaneously in a SCPT. Further, one can obtain additional information by analyzing the seismic motion measured in three orthogonal receiver-components (thus, P-, S-, and converted waves) and addressing frequency-dependent seismic wave propagation over a broad frequency range. This will provide important static and dynamic soil properties (e.g., texture, in situ stress, fluid-flow properties like viscosity, porosity and permeability). The present research is focused on these possibilities. The goal was to develop a reliable SCPT system including an array of 3C seismic sensors, which is coupled with broadband, controlled, repeatable vertical and horizontal seismic sources.

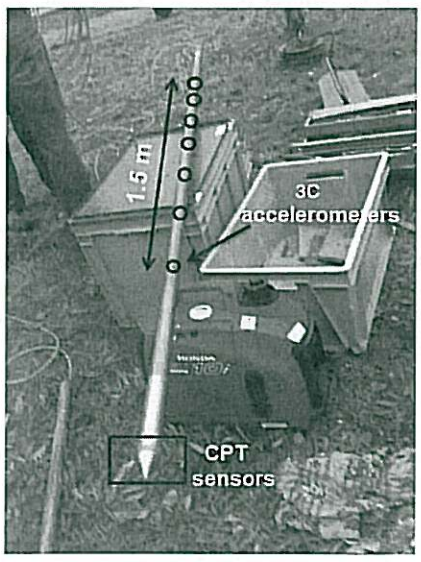

Figure 1. Digital 3C array SCPT downhole system.

In the following sections, we shall first discuss the array 3C seismic cone penetrometer developed in this research. Then we shall illustrate results of two shallow-depth field experiments and examine the frequency band and the quality of the recorded data for impulsive and vibratory seismic sources. Finally, we look at the fine-scale V_S profiles and the depth-specific estimation of dispersive seismic velocity and attenuation, using downhole array-seismic data.

THE DIGITAL ARRAY 3C SEISMIC CONE PENETROMETER

Here, we present the array-seismic sensor assembly, the SCPT data acquisition and field quality-control system, and the seismic sources that can be used with this system. Figure 1 shows a photo of the downhole system. The digital 3C seismic array is attached above a class 1 24-bit digital CPT cone of high accuracy.

Digital array 3C seismic sensor assembly

The system is designed considering the technical requirements (e.g., sensitivity, frequency response, anticipated wave velocities and polarizations, sensor coupling, temporal and spatial sampling, use with impulsive and vibratory sources), the practical feasibility aspects, and the research goals. The aim is to sample densely in depth and with high precision the full-elastic (3C) wavefield due to a given seismic source. At the same time, the total length of the seismic array should not be too long for it to be a handy and easily manageable field system. The coupling of the 3C seismic sensors inside the tool has to be strong and as uniform as possible in azimuth and between the depth levels to receive the elastic wavefield undistorted and over a wide frequency range. The depth-sampling should be high enough to allow recording of spatially unaliased data in the low-velocity soil layers. The temporal sampling has to be high enough to be able to measure realistic small changes in seismic velocity over the length of the seismic array, even for high-velocity P-waves. The main research-related goals are capacity to capture reliably the dispersive nature of seismic wave velocity and attenuation in the near-surface soil layers to address the in situ fluid-flow properties, in situ stress (and anisotropy), and the mechanical properties (including the link between q_c and V_S). Meeting all these targets has proved challenging; consequently, the design parameters are optimized through a series of iterations.

The final seismic sensor array, 1.5 m in total length, is made of seven modules — each housing one 3C MEMS accelerometer (Figure 1). The diameter of the cylindrical seismic array is 35.7 mm, which is a standard in CPT. The 60° digital cone used has a 10 cm^2 projected cone area. The distance from the tip of the cone to the lowest seismic sensor is 0.5 m. The length of the total system, including the digital cone and the seismic array, is 2.19 m. The distance between two successive accelerometers is 0.25 m. Considering the spatial aliasing limit of $V_{min}/2f_{max}$, where V_{min} is the minimum phase velocity of a wave incident to the array, and f_{max} is the maximum frequency, 0.25 m receiver spacing implies that for a shear wave with a phase velocity as low as 100 m/s, we can record up to 200 Hz without aliasing. In the case of 200 m/s

Downloaded 27 Apr 2012 to 131.180.60.197. Redistribution subject to SEG license or copyright; see Terms of Use at http://segdl.org/

velocity, the maximum recordable frequency is 400 Hz. For the typical frequencies and propagation velocities of shear waves in soft soils, the 1.5-m length of the downhole receiver array corresponds to 0.5–2.0 times the wavelength, which is a reasonable distance for a stable distinction of velocity and attenuation changes.

MEMS accelerometers are compact, low-power, triaxial, inertial sensors, which combine micromachining and integrated circuit technology. They are known for their reliability and ruggedness. The accelerometer that we have used has a flat frequency response up to 2 kHz (where the first resonance occurs). The maximum possible time sampling is 5 kHz (f_{Nyquist}), i.e., 0.1 ms minimum sample interval. The capacity and the speed of the memory chip determine this limit.

Each accelerometer, along with other electronics, is mounted on a printed circuit board, which is fixed within a cylindrical metal housing. This metal housing, in turn, is locked to the inside wall of the seismic cone module by means of screws applying pressure that is very nearly uniform in the azimuthal plane. The modular structure of the seismic sensor array offers flexibility and easy handling. For trouble shooting, a faulty module can be replaced by a good one without affecting the functionality of the others. The modules are connected to each other through special connectors that ensure that the orientations of the 3C accelerometer is identical at all seven depth-levels in the array.

SCPT data-acquisition system

Digital data from seven 3C accelerometers (total 21 channels, plus three extra channels for source monitoring) together with digital CPT data (q_c, f_s, u, I) are transferred serially through a cable to a laptop computer that serves as the SCPT data-acquisition system. The source reference signal in the case of a vibratory source, generated from data of multiple sensors placed on/in the source, is used to perform crosscorrelation or deconvolution of the raw vibrograms. Frequency filtering and several modes of display are possible for quality control in field. Acquisition parameters (e.g., gain or amplification for accelerometer channels, time sampling, trace length, source type, etc.) are assigned in this system. Digital CPT data are stored and displayed here.

Seismic sources

Impulsive and vibratory sources can be used with this 3C array SCPT system. The preferred sources are high-frequency vibrators that are suitable for high resolution near-surface investigations (e.g., Ghose et al., 1996; 1998). This is because of the controlled nature of these sources (thus offering the possibility to compensate for the loss of higher frequencies through use of nonlinear sweep), broad frequency bandwidth, and a relatively accurate source monitoring (enabling source signature deconvolution for amplitude fidelity and minimum source-to-source variations). The impulsive sources can be of any kind; we have so far used the vertical hammer and the weight-drop sources for the compressional wave and the sledge hammers for the shear wave. The trigger signal from the source activates the downhole sensors as well as the acquisition system to synchronize the starting time.

The cone is pushed into the ground by means of a hydraulic ram system, which is wheel-mounted for ease in mobility in the field.

FIELD EXPERIMENTS

Here, we discuss the performance of the 3C array-SCPT system using data sets from two shallow-depth experiments performed at a given site. In the first experiment, only sledge hammer source is used. In the second experiment, sledge hammer and vibratory shear-wave sources as well as a vertical hammer as the compressional-wave source are used to acquire 9C (three source- and three receiver-components) downhole seismic data. In addition to the downhole measurements, in the second experiment, for the same shots 3C surface geophone data are acquired along a line passing through the SCPT location.

The test site is made of a sandy top surface overlying the Holocene clay and sand layers that extend to the Pleistocene sand appearing at 6–7 m depth. The Pleistocene sand is very stiff and pushing the cone is difficult with our hydraulic rams and anchor system. Consequently, our present experiments are restricted to the top several meters of the subsurface. The SCPT system can, of course, be used to greater depths in cases in which the cone can be pushed deeper into the ground. The results presented here are sufficient for evaluation of the functionality of the array-SCPT system and the data quality.

Array-SCPT experiment one

A wooden sledge hammer source is placed as close as possible (90 cm) from the SCPT location. The water table is at about 1.25 m. The cone tip is first pushed to 1.7-m depth (below the water table) while acquiring CPT data (q_c, f_s, u, I), and then the penetration is stopped for acquiring seismic data. In this experiment, the time sampling for the accelerometer data is 0.2 ms ($f_{\text{Nyquist}} = 2500$ Hz). For every strike of the sledge hammer, 21 seismic traces from seven 3C accelerometers are acquired. The orientation of the x- and y-components are identical at all depths within the array. Every shot is repeated two to four times for subsequent vertical stacking. The cone is then pushed into the ground an additional 1 m while acquiring the CPT data, and the penetration is again stopped for seismic data acquisition. This process is repeated. The seismic array is 1.5-m long, and because we stop at every 1 m, we have three depth levels where the acceleration is measured twice. Repeating one receiver point is normally sufficient, but in this test, we have taken three depth-levels that overlap, for checking purposes. The arrival times are found to be quite repeatable. This allows for high-quality velocity estimation. Figure 2a shows 3C accelerometer data for the sledge hammer shear wave source (right hammer strike). Note the clean shear wave arrivals in the horizontal (x, y)-components. Some compressional wave has been generated by the shear source; this is visible in the vertical (z) component. The energy is mainly distributed in the x- and y-components, as expected.

The x- and y-components have been rotated to maximize energy within a time window in one rotated component and minimizing simultaneously in the other component. A fixed-length time window is chosen automatically around the peak signal amplitude in the raw data. If two orthogonal shear sources are used, then one can perform a 4C rotation (Alford, 1986) to correct for anisotropy. Figure 2b shows the result of 2C rotations for left and right hammer strikes. The polarity of the recorded direct wave is reversed between left and right hammer strikes, indicating horizontally polarized shear waves. The amplitude decay of the shear wave with depth

Downloaded 27 Apr 2012 to 131.180.60.197. Redistribution subject to SEG license or copyright; see Terms of Use at http://segdl.org/

in soft soil is conspicuous. Vertical source stacking is necessary to enhance the signal-to-noise ratio (S/N) at greater depths.

Array-SCPT experiment two

This experiment is carried out several months after the first one. During this period, the 3C array SCPT system is further improved. Three different seismic sources are used. Two shear sources — a sledge hammer and a vibrator — are placed across each other on two sides of the SCPT. A vertical hammer compressional source is located at 90° from the shear sources. The distance of the vibrator and the sledge hammer from the SCPT location is 90 cm. This distance is 75 cm for the vertical hammer.

The vibratory shear source used here is a high-frequency, electromagnetic vibrator developed earlier for high-resolution near-surface applications (Ghose et al., 1996; Brouwer et al., 1997). It is a 70 cm × 35 cm × 30 cm box that houses an electromagnetic shaker. Linear, nonlinear, and coded sweeps can be generated. This source is about 100 kg in total weight and can generate a maximum shear force of 500 kN on the ground. The operational frequency bandwidth (limited by the resonances) is 10–450 Hz, although it is possible to run the source at much higher frequencies. In near-surface soft soils where V_S is often very low (70–150 m/s in clay-peat-sand layers), such high-frequency shear waves offer very short (less than a meter) wavelengths and hence, resolution of a few decimeters. Nonlinear sweeps can be designed to compensate for the loss of higher frequencies in the ground, thereby achieving much higher resolution than the impulsive shear wave sources. Significant efforts were made earlier to ensure a good monitoring of the source (baseplate and reaction mass) motions, including vibrator-ground coupling, over the entire operational frequency bandwidth. Because of this possibility, the deterministic source signature deconvolution (instead of crosscorrelation) is performed to remove the source function (including source coupling) during raw vibrogram compression (Ghose, 2002). This provides good amplitude fidelity, reduces problems due to source-to-source coupling variation, and improves separation of events in the shear wave reflection data.

To use this high-frequency shear wave vibrator together with the 3C array SCPT system, special adaptations are made in the SCPT hardware and the acquisition system. These adaptations make it possible to use for SCPT and also the high-frequency compressional-wave vibrator (Nijhof, 1989; Ghose et al., 1998).

At first, the cone tip is pushed to 1.5 m depth into the ground so that the pore-pressure sensor is below the water table. At that depth, the penetration is stopped and the first set of seismic array data is acquired using different sources. If the cone is stopped at a depth above the water table, then the oil-filled porous membrane of the pore-pressure sensor can get clogged (though other sensors of the SCPT system will work fine). Therefore, for good pore-pressure measurements, it is important to start acquiring seismic data only after the pore-pressure sensor has reached the water table. However, if pore-pressure measurement is done separately or is not necessary, then one can start acquiring seismic data right from the surface level. Subsequently, the cone is pushed downward by another 1.25 m while collecting CPT data, and then stopped to acquire the array seismic data. This process is repeated. In this experiment, for checking purposes, we have an overlap of two depth points between successive depth arrays. However, in practice, a one-point overlap is sufficient, and hence, pushing the cone every time by 1.5 m is justified.

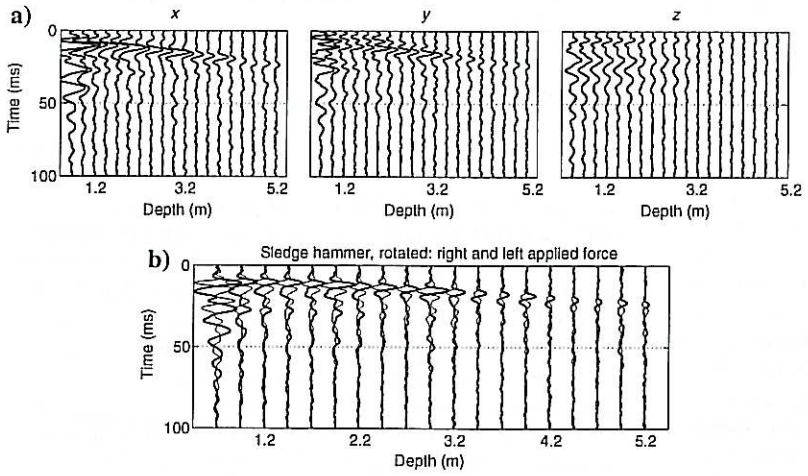

Figure 2. Experiment 1: (a) 3C accelerometer data from the digital array-SCPT system, with sledge hammer shear wave source. Vertical stack count is two. A single scaling factor is applied for all 3 panels. (b) Same data after rotation of the x- and y-components. The thick and thin lines correspond to right and left hammer strikes for the source, respectively.

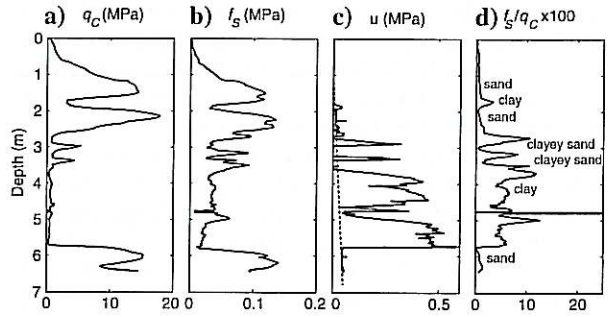

Figure 3. Experiment 2: Digital cone data from array-SCPT: q_c is cone tip resistance, f_s is sleeve friction, and u is pore pressure. The friction ratio (f_s/q_c) is sensitive to changes in soil composition. The soil layer composition is marked in (d).

Figure 3 shows the acquired digital CPT data. From 0 to 3.5 m depth, there is an intercalation of sandy and clayey layers, corresponding to high and low q_c values, respectively. Between 3.5 and 5.7 m, it is primarily clay. The Pleistocene sand appears at 5.7 m. The clay layers are better discernible in the friction ratio (f_s/q_c) profile. The pore pressure (u) follows hydrostatic gradient in the sandy zones (dotted line in Figure 3c).

Figure 4a shows the 3C downhole accelerometer data (frequency pass band 15–250 Hz) for the sledge hammer and shear wave vibrator. In these plots, a single scaling factor is used for x-, y-, and z-components. The vertical stack count is two for both sources.

Downloaded 27 Apr 2012 to 131.180.60.197. Redistribution subject to SEG license or copyright; see Terms of Use at http://segdl.org/

The redundant traces (at the overlap between two successive arrays) are eliminated. The raw vibrator data are deconvolved using the groundforce estimated from the carefully measured source motion. A vibrator sweep length of 3.7 s and a record length of 4.2 s has resulted in a deconvolved trace length of 500 ms. The first 150 ms of data is shown here. Evidently, the shear wave vibrator has a much higher S/N than the sledge hammer (Figure 4a). At greater depths, the shear-wave arrivals are more visible for the vibrator. The S/N and depth of penetration can be improved, for both sources, through source stacking. As in the first experiment, we notice that the shear sources also have generated some compressional waves, visible in the z-component. The phase of the source wavelet is, as expected, different between vibrator and the sledge hammer: the vibrator has a zero-phase wavelet, and the hammer has a mixed-phase wavelet. There appears to be a small static shift in the absolute arrival time between hammer and vibrator data, the reason is not obvious; however, this will not affect the velocity and the attenuation estimates based on the seismic array data.

The result of 2C rotation of the downhole accelerometer data with the surface shear wave vibrator source is shown in Figure 4b. The rotated traces for left and right initial displacements of the vibrator are plotted. The arrival of horizontally polarized shear wave is unambiguous, as we notice clear polarity reversal. The vibrator source wavelet appears to be very similar at all depths, indicating the benefit of deterministic source signature deconvolution.

In the case of a vibrator, it is possible to control the source spectrum. We wanted to test if the observed S-wave frequency band in soft soil can be pushed from low to high frequencies (exceeding 200 Hz) with the vibrator. Consequently, the used shear wave vibrator sweep is from 100 to 450 Hz (linear), although ideally, one should us a broader vibrator sweep (starting at a lower frequency) for a greater penetration depth and a broadband response. In Figure 5, the common source gathers (pass band 15–250 Hz), for two different shear sources — sledge hammer and vibrator — are shown. In Figure 5a, the array seismic data for the depth range of 1.0–2.5 m are shown. The average amplitude spectrum for the array of seven traces is illustrated on the right. In Figure 5b, the array data for the depth range of 2.75–4.25 m, along with the average amplitude spectra, are shown. For the two sources, the receivers including the receiver coupling, are identical. We notice that for the sledge hammer, the amplitude sharply drops beyond 150 Hz; however, for the controlled, shear wave vibrator, the amplitude remains high until the limit of the pass band used, i.e., 250 Hz. Such high-frequency shear waves in soft soil correspond to very small wavelengths. A relatively broadband seismic data can thus be acquired with the array seismic cone, when used in conjunction with the vibratory

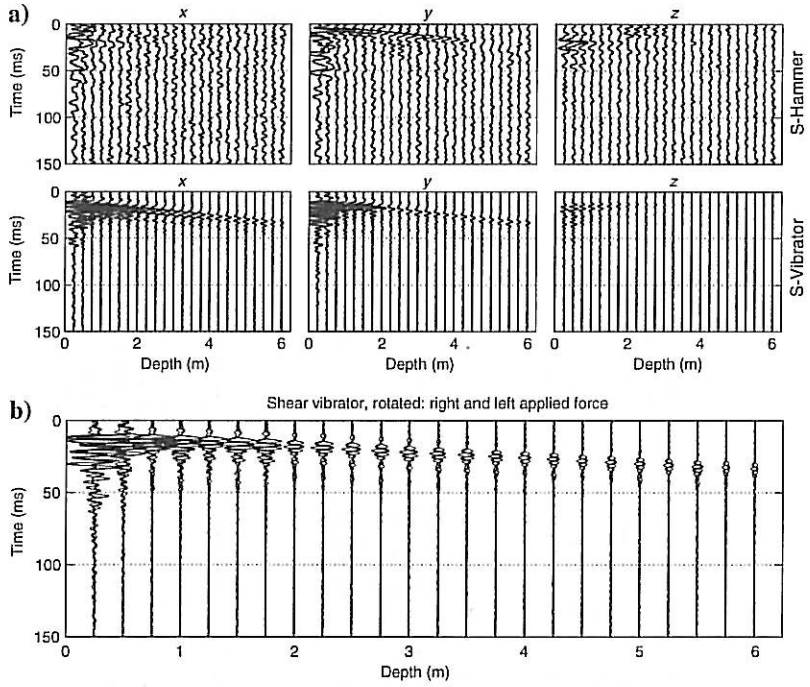

Figure 4. Experiment 2: (a) 3C accelerometer data from the digital array-SCPT system, with sledge hammer (impulsive) and shear wave vibrator sources. (b) Shear wave vibrator data after rotation of the x- and y-components. The thick and thin lines correspond, respectively, to right and left hammer strikes for the source.

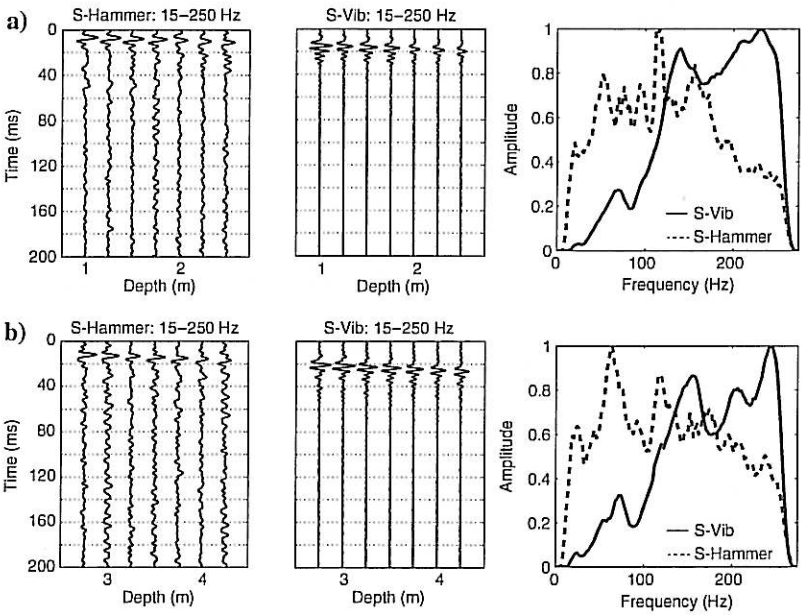

Figure 5. Experiment 2: Seismic array data (downhole common source gather) with sledge hammer and shear wave vibrator sources (vibrator sweep 100–450 Hz), for two depth ranges: (a) 1.0–2.5 m and (b) 2.75–4.25 m. The average amplitude spectrum of all seven traces is shown on the right.

Downloaded 27 Apr 2012 to 131.180.60.197. Redistribution subject to SEG license or copyright; see Terms of Use at http://segdl.org/

source. This is advantageous in studying frequency-dependent wave propagation in soil.

The full potential of SCPT can be used when downhole 3C seismic data are available for 3 different source components — two mutually orthogonal horizontal sources (H1 and H2) and one vertical source (V). So far, it has not been easy to acquire high-quality 9C downhole data in soft soil. However, the information that can be extracted from such data sets are significant. Figure 6 shows 9C data acquired with the digital array-SCPT system. Here, data from a single depth-array (4.5–6.0 m) are illustrated for H1, H2, and V source types (frequency pass band 15–250 Hz for H1 and H2, and 15–350 Hz for V). A shear wave vibrator is used for HI and H2. For V, the source is a vertical hammer. The stack count for V is four, for H1 and H2 it is two and one, respectively. In these plots, the scaling factor is constant for x-, y-, and z-components. The distribution of energy in different receiver components for different source types is justifiable. Good data quality, a constant source function for the receiver array, and the dense depth sampling collectively add to the value of the 9C data set.

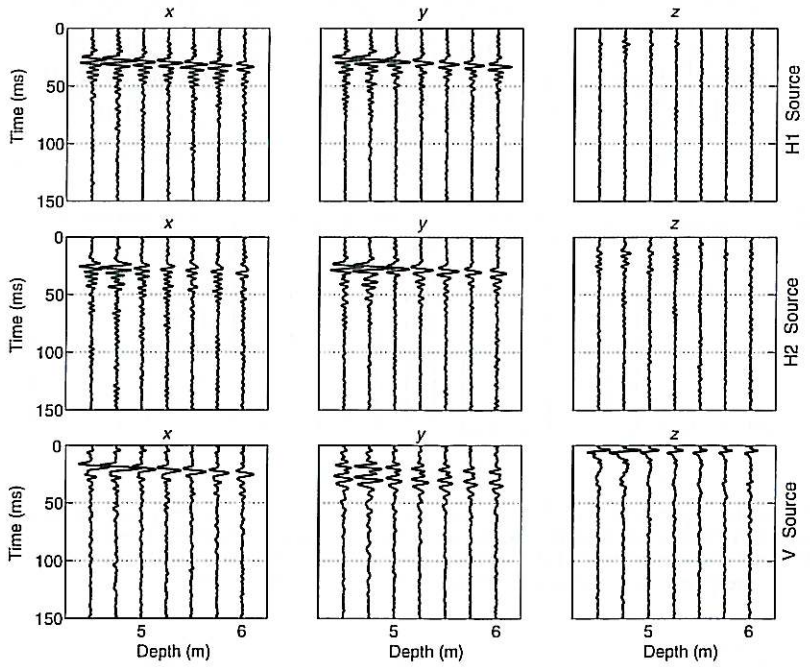

Figure 6. Experiment 2: 9C seismic array data (common source gather). Array depth: 4.5–6.0 m.

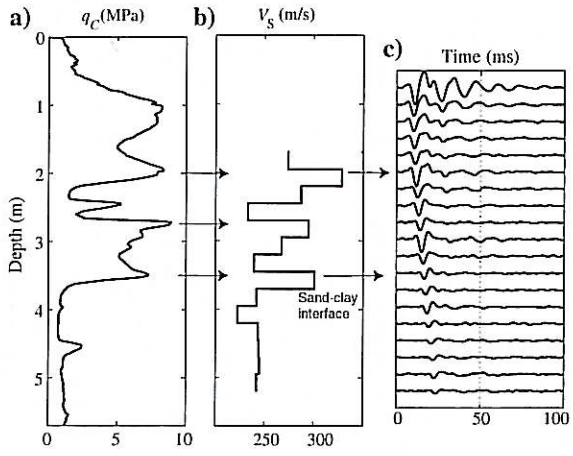

Figure 7. Experiment 1: (a) q_c profile, (b) V_S profile obtained by crosscorrelation of traces (shear wave window) at two adjacent depth levels. The shear wave source is sledge hammer. Note the correspondence between q_c and V_S depth profiles (arrows). (c) Downhole seismic data.

FINE-SCALE V_S PROFILES AND THE ESTIMATES OF SEISMIC DISPERSION IN SOIL FROM ARRAY-SCPT

V_S profile and correlation with q_c

The crosscorrelation of the shear wave first arrival between two adjacent depths in the downhole seismic array has been found to provide stable estimates of V_S. A time window of a fixed width, chosen automatically around the peak amplitude, is used to perform the crosscorrelation. Figure 7b shows the interval V_S (25 cm interval) estimated from the rotated horizontal-component seismic data from the first experiment (Figures 2b and 7c). In Figure 7a, q_c from the same SCPT is shown. Note the good correspondence in depth between the changes in q_c and that in V_S, in a fine scale (25 cm). The stronger parts (higher q_c), corresponding to sandy layers, show high V_S, whereas the softer (lower q_c) clayey parts show low V_S. Such fine-scale correlation in depth between V_S and q_c was not reported earlier.

In the case of SCPT, as the cone is pushed into the soft soil, the seismic receiver coupling is usually very good. Additionally, in the case of an array SCPT as we use here, the source function is constant for the array. This is the reason why the extracted V_S field, although exhibiting a relatively large fluctuation in depth distribution, matches remarkably well with the q_c depth profile (Figure 7) and, therefore, appears to be a true representative of the heterogeneity distribution in the subsoil.

Figure 8b shows interval V_S estimated by crosscorrelation from the rotated horizontal-component seismic data of the second experiment (Figure 4b). For multiple source stacking, the crosscorrelation has been done separately, to check the reproducibility. The estimated V_S values are robust. In Figure 8a, the q_c profile from the same SCPT is shown. There is again a general correlation between V_S and q_c depth profiles. If corrected for the pore-pressure and the effective vertical stress, this correlation is expected to improve further, as reported earlier (e.g., Simonini and Cola, 2000).

The correlation between V_S and q_c depth profiles explains earlier observed correspondence between the subsoil interfaces encountered in CPT and the reflections seen in surface shear wave reflection data (Ghose et al., 1996, 2002; Brouwer et al., 1997; Jarvis and Knight, 2000; Ghose and Goudswaard, 2004; Knight and Pidlisecky, 2005). In Figure 8c, a shear wave reflection shot gather acquired along a line passing through the SCPT location of the

Downloaded 27 Apr 2012 to 131.180.60.197. Redistribution subject to SEG license or copyright; see Terms of Use at http://segdl.org/

second experiment is shown. The sledge hammer source is located at 90 cm from the SCPT location and 2 m from the first geophone on the surface line; the geophone interval is 0.75 m. Two-way time has been converted to depth using V_S from SCPT for the shallowest part and $V_S = 350$ m/s assumed for the Pleistocene sands (depth > 6 m). Note the strong reflection event at around 6–7 m depth in Figure 8c. This is probably the Holocene-Pleistocene (clay-to-sand) boundary seen in CPT. The very shallow sand-to-clay boundary at about 3 m is probably also a reflector, but it is less distinct in the surface seismic shot gather.

Additionally, V_S and q_c correspond to very different strain levels and, hence, very different soil properties (elastic stiffness versus strength). The observed correlation between V_S and q_c in sands results from the common dependence of the two on the effective stresses and the relative density ($D_R = (e_{max} - e)/(e_{max} - e_{min})$, where e is in situ void ratio and e_{max} and e_{min} are, respectively, maximum and minimum void ratios). The depth distribution of the ratio of small strain shear modulus G_0 ($G_0 = V_S^2\rho$, where ρ is bulk density) to q_c has been reported to have a good correlation with the depth distribution of D_R in clean sand (e.g., Baldi et al., 1988). A low D_R corresponds to a high G_0-to-q_c ratio, and vice-versa. The fine-scale, stable $V_S - q_c$ depth correlation that we now extract from the array SCPT data can be useful in predicting the variation of in situ D_R in sandy soils. Although D_R is an indicator of the state of compaction of sand and is a crucial parameter in geotechnical engineering, it is practically impossible to obtain in situ distribution of D_R in granular (sandy) soil in a non-invasive manner.

Estimates of seismic dispersion

Shallow subsoil is porous. The propagation of seismic waves is governed by poroelasticity. Due to poroelasticity, the velocity and attenuation of seismic waves are frequency-dependent. Dispersive seismic velocity and attenuation contain information of the fluid-flow properties (e.g., porosity, permeability, viscosity). Recently, it has been shown that seismic dispersion, in the low-frequency range typical of field-seismic data, can be used to estimate in situ flow properties in soils (Zhubayev and Ghose, 2011, 2012). Digital 3C array-seismic data are useful in evaluating frequency-dependent wave propagation in soil. Because the seismic source function is constant in a receiver array, the dispersive velocity and attenuation, estimated over the array length, are more reliable. Additionally, the use of vibratory sources offer high-quality data with a much broader frequency bandwidth than the impulsive sources, which is advantageous for dispersion studies.

Figure 9 illustrates the estimation of seismic dispersion using the receiver array data from SCPT. Downhole shear wave data (rotated horizontal components from the second experiment), for the depth range of 1.5–3.0 m, are shown in Figure 9a. The phase difference $\Delta\phi(\omega)$ between two traces within an array, for a given frequency ($\omega = 2\pi f$), is used to estimate the velocity ($V(\omega) = \Delta x/\Delta t = \Delta x\omega/\Delta\phi(\omega)$). From the array of seven seismic receivers, the top

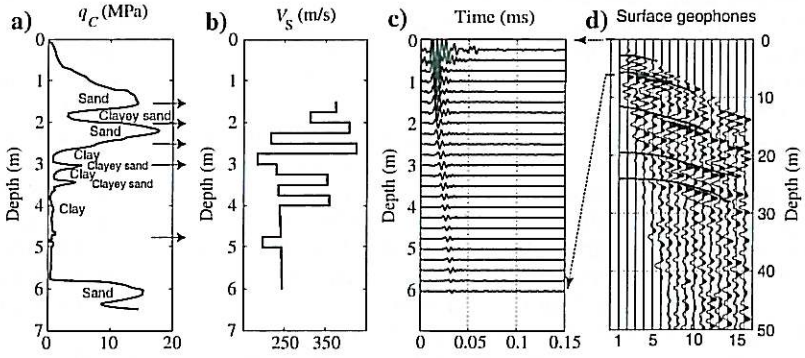

Figure 8. Experiment 2: (a) q_c profile (b) V_S profile obtained by crosscorrelation of traces (shear wave window) at two adjacent depth levels. Shear wave source is vibrator. Arrows mark the general correspondence between q_c and V_S depth profiles. (c) Surface seismic reflection shot gather (horizontal component geophones in crossline orientation) along a line passing through the SCPT location.

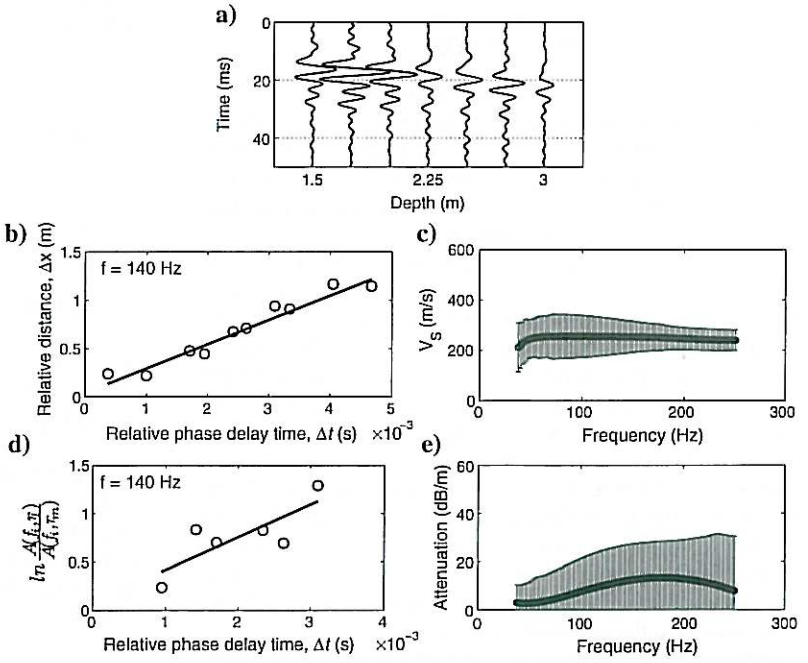

Figure 9. Experiment 2: Estimating effective dispersion in soil from the array seismic data from SCPT. (a) Array seismic data, (b) seismic velocity for a given frequency (140 Hz for this illustration) estimated from the slope of the best-fit straight line in the distance versus phase delay-time plot for multiple pairs of traces in the seismic array, (c) velocity dispersion curve with the standard deviations (vertical bars), (d) seismic effective attenuation for a given frequency (140 Hz) estimated from the slope of the best-fit straight line in the spectral amplitude ratio versus relative phase delay-time plot for multiple pairs of traces in the seismic array, and (e) dispersive effective attenuation curve with the standard deviations (vertical bars).

Downloaded 27 Apr 2012 to 131.180.60.197. Redistribution subject to SEG license or copyright; see Terms of Use at http://segdl.org/

one is taken first as the reference, and the phase difference between the reference and all other receiver traces in the array are estimated. Next, the lowest receiver is taken as the reference, and again the phase differences are obtained. The Δt is calculated from $\Delta\phi$. Finally, from the slope of the best-fitting straight line in $\Delta x - \Delta t$ plot, the velocity is estimated (Figure 9b). Any anomalous Δt value is automatically eliminated. Because we use downhole array-seismic data, the average velocity over the array length (1.5 m) is determined using many receiver combinations, this offers added stability to the estimated velocity. The procedure is repeated for all frequencies to get the effective velocity dispersion curve, as shown in Figure 9c. Here, the vertical bars indicate the standard deviations. For estimating attenuation, the spectral ratio method is used, but in stead of using only two receivers at two different depths, again, all the receivers in the array are used and the top and the bottom receivers are taken as the reference ones. Using multiple receivers is critically important for the reliability. Any anomalous amplitude is automatically discarded. The slope of the best-fitting line in the spectral amplitude ratio versus Δt plot gives the inverse quality factor Q^{-1} for shear wave (Figure 9d), from which the attenuation coefficient α is obtained ($\alpha = 8.686\pi f Q^{-1}/V(f)$ dB/m). The procedure is repeated for all frequencies to get the frequency-dependent effective attenuation, as illustrated in Figure 9e. The standard deviation is indicated by the vertical bars. We have checked that the dispersive velocity and attenuation estimates using the array seismic data from SCPT are quite robust. It is possible to obtain intrinsic dispersion by subtracting the effect of multiple scattering from the effective dispersion estimated as above.

DISCUSSION

The difference in the received wavefield due to changes in the seismic source function is usually significant. If the source function is different for different receivers, then that difference negatively influences the evaluation of the interval properties, e.g., velocity and attenuation. The result of crosscorrelation to find the traveltime or the estimation of spectral amplitude ratio to derive the seismic attenuation between two receiver depths are greatly affected. The advantage of having a downhole seismic receiver array, instead of only one or two receivers, is that the source function is constant for the entire array. This is a good reason why the derived velocity profile appears to be more reliable when we use the seismic array in SCPT, because it reveals a remarkable fine-scale correlation between V_S and q_c depth profiles (e.g., in Figure 7). Of course, there will still be the receiver coupling variations; however, the receiver coupling is much better in SCPT compared to VSP, as in CPT the coupling with the surrounding soil is good and uniform. Nevertheless, having multiple receivers in an array, this receiver coupling variation can be addressed in a statistical manner. This has been done in estimating seismic dispersion (Figure 9). With only one or two receivers, the uncertainty is large.

High-quality data, including constant source function within the receiver array and densely sampled full-elastic wavefield, contain much information of the shallow subsoil, e.g., anisotropic stress and fluid-flow properties. Furthermore, the array seismic data can be acquired in time-lapse mode to monitor changes in the subsoil, e.g., change in the in situ state of stress (Ghose, 2010).

In the present system, array seismic data and data from the CPT sensors are transferred serially from the downhole unit to the acquisition system. For an impulsive source, the seismic trace is short and the data transfer is quick. But for the vibratory source, the raw traces are long, and consequently, the serial data transfer takes a few minutes per shot. In the case of source stacking, this takes a long time. This should be a subject for improvement in the future. Use of fiber optics or cable-free technology may provide the solution.

The finest possible temporal sampling for seismic data is now 0.1 ms (f_{Nyquist} 5 kHz). For shear wave, which has a low velocity in soft soil, this time sampling is sufficient for a stable resolution of the arrival-time difference between the sensors. For a compressional wave, however, one will ideally like to have even finer sampling than 0.1 ms for good results. A different MEMS sensor with higher speed and larger memory, yet satisfying the size constraints, if available, can help to achieve this goal.

The shear wave vibrator that has been used in the second experiment, in general, offers a broader frequency band than a sledge hammer (see also Ghose and Goudswaard, 2004). Because in this case, the source motion can be reliably monitored, the deterministic source signature deconvolution is performed for compressing the raw vibrograms. In our experiment, we have used a vibrator sweep that is linear from 100 to 450 Hz. To take the full advantage of a high-frequency vibrator, one should, however, use a nonlinear sweep with a broader frequency band.

CONCLUSIONS

The digital 3C array-seismic cone penetrometer can improve and extend the utility of the traditional SCPT. In the downhole tool, seven MEMS-based digital triaxial accelerometers, which are known for their ultracompact size, low power consumption, reliability, and ruggedness, are aligned at 0.25-m intervals. These seismic sensors have a flat response up to 2 kHz. The length of the 3C seismic array is 1.5 m. The highest time-sampling frequency f_{Nyquist} is presently 5 KHz. This seismic array is attached to a class 1 digital seismic cone that measures cone tip resistance q_c, sleeve friction f_s, pore-pressure u, and inclination I. A dedicated acquisition system for this array SCPT tool has been developed. This downhole 3C array can be used together with impulsive seismic sources and vibratory sources.

Results from two field experiments show that the data quality is very good. When coupled with a high-frequency, controlled vibratory source, the data quality, the frequency bandwidth and the scope of applicability are further improved. Reliable estimation of the V_S profile is possible. A correlation, even in a fine scale, between V_S and q_c depth profiles could be observed. The high-quality array seismic data are also useful in estimating dispersive seismic velocity and attenuation, which contain information of the in situ fluid-flow properties in the poroelastic soil layers. The digital 3C array SCPT is expected to be a powerful supplement to the high-definition near-surface imaging, characterization and monitoring tools that exist now.

ACKNOWLEDGMENTS

This project is financially supported by the Dutch Technology Foundation STW, applied science division of NWO, the technology program of the Ministry of Economic Affairs (grant DAR.5761). The 3C array-SCPT system is designed and manufactured in cooperation with the company A.P van den Berg. The contribution of Nico Koster and Erik Landskroon is acknowledged. Alimzhan Zhubayev has helped in data processing. Han de Visser and Alber

Downloaded 27 Apr 2012 to 131.180.60.197. Redistribution subject to SEG license or copyright; see Terms of Use at http://segdl.org/

Hemstede are acknowledged for their assistance in the field experiments.

REFERENCES

Alford, R. M., 1986, Shear data in the presence of azimuthal anisotropy: Dilley, Texas: 56th Annual International Meeting, SEG, Expanded Abstracts, 476–479.

Andrus, R. D., P. Piratheepan, B. S. Ellis, J. Zhang, and C. H. Juang, 2004, Comparing liquefaction evaluation methods using penetration-V_S relationships: Soil dynamics and earthquake engineering, **24**, 713–721, doi: 10.1016/j.soildyn.2004.06.001.

Baldi, G., R. Bellotti, V. N. Ghionna, M. Jamiolkowski, and D. C. F. Lo Presti, 1989, Modulus of sands from CPT and DMT: Proceedings, 12th International Conference on Soil Mechanics and Geotechnical Engineering, **1**, 165–170.

Baldi, G., D. Bruzzi, S. Superbo, M. Battaglio, and M. Jamiolkowski, 1988, Seismic cone in Po River sand: Penetration testing: Proceedings, 1st International Symposium on Penetration Testing, 643–650.

Brouwer, J., R. Ghose, K. Helbig, and V. Nijhof, 1997, The improvement of geotechnical subsurface models through the application of S-wave reflection seismic exploration: 3rd Annual Meeting, EEGS, Extended Abstracts, 103–106.

Butcher, A. P., and J. J. M. Powell, 1995, Practical considerations for field geophysical techniques used to assess ground stiffness: Proceedings International Conference on Advances in Site Investigation Practice, 701–714.

Campanella, R. G., and P. K. Robertson, 1984, A seismic cone penetrometer to measure engineering properties of soil: 54th Annual International Meeting, SEG, Expanded Abstracts, 138–141.

Campanella, R. G., P. K. Robertson, and D. G. Gillespie, 1986, Seismic cone penetration test: Proceedings of In Situ '86, 116–130, ASCE.

Eslaamizaad, S., and P. K. Robertson, 1998, Cone penetration resistance of sand from seismic tests, *in* P. K. Robertson, and P. W. Mayne, eds., Geotechnical site characterization: Balkema, 1027–1032.

Ghose, R., 2002, High-frequency shear wave reflections from shallow subsoil layers using a vibrator source: Sweep cross-correlation versus deconvolution with groundforce derivative: 72nd Annual International Meeting, SEG, Expanded Abstracts, 1408–1411.

Ghose, R., 2010, Estimating in situ horizontal stress in soil using V_S time-lapse measurements, *in* R. D. Miller, J. H. Bradford, and K. Holliger, eds., Advances in near-surface seismology and ground-penetrating radar: SEG, 131–152.

Ghose, R., F. Almeida, H. Hermosilha, F. Bonito, and C. Cardoso, 2002, Shallow S-wave reflections over lagoon deposits: 8th Annual Meeting, EEGS, Extended Abstracts, 9–12.

Ghose, R., J. Brouwer, and V. Nijhof, 1996, A portable S-wave vibrator for high-resolution imaging of the shallow subsurface: 58th Annual International Conference and Exposition, EAGE, Extended Abstracts, M037.

Ghose, R., and J. Goudswaard, 2004, Integrating S-wave seismic-reflection data and cone-penetration-test data using a multiangle multiscale approach: Geophysics, **69**, 440–459, doi: 10.1190/1.1707064.

Ghose, R., V. Nijhof, J. Brouwer, Y. Matsubara, Y. Kaida, and T. Takahashi, 1998, Shallow to very shallow, high-resolution reflection seismic using a portable vibrator system: Geophysics, **63**, 1295–1309, doi: 10.1190/1.1444431.

Hegazy, Y., and P. W. Mayne, 1995, Statistical correlations between V_S and cone penetration test data for different soil types: Proceedings, 2nd International Symposium on Cone Penetration Testing, **2**, 173–178.

Jarvis, K. D., and R. Knight, 2000, Near-surface VSP surveys using the seismic cone penetrometer: Geophysics, **65**, 1048–1056, doi: 10.1190/1.1444798.

Knight, R., and A. Pidlisecky, 2005, Cone-based geophysical imaging: A proposed solution to a challenging problem: The Leading Edge, 34–38, doi: 10.1190/1.1859698.

LeBlanc, A.-M., R. Fortier, C. Cosma, and M. Allard, 2006, Tomographic imaging of permafrost using three-component seismic cone-penetration test: Geophysics, **71**, no. 5, H55–H65, doi: 10.1190/1.2235876.

Lunne, T., P. K. Robertson, and J. J. M. Powell,1997, Cone penetration testing in geotechnical practice: Blackie Academic Professional.

Mayne, P. W., and G. J. Rix, 1993, G_{max}-q_c relationships for clays: Geotechnical Testing Journal, **16**, 54–60, doi: 10.1520/GTJ10267J.

McGillivray, A. V., 2007, Enhanced integration of shear wave velocity profiling in direct-push site characterization: Ph.D. thesis, Georgia Institute of Technology.

Nijhof, V., 1989, A portable high-frequency vibrator for high-resolution shallow seismic profiling: 59th Annual International Meeting, SEG, Expanded Abstracts, 670–673.

Robertson, P. K., 1982, In-situ testing of soil with emphasis on its application to liquefaction assessment: Ph.D. thesis, University of British Columbia.

Robertson, P. K., R. G. Campanella, D. Gillespie, and A. Rice, 1986, Seismic CPT to measure in situ shear wave velocity: Journal of Geotechnical Engineering, **112**, 791–803, doi: 10.1061/(ASCE)0733-9410(1986)112:8(791).

Schneider, J. A., A. V. McGillivray, and P. W. Mayne, 2004, Evaluation of SCPTU intra-correlations at sand sites in the lower Mississippi River Valley, USA: 2nd International Conference on Site Characterization, **2**, 1003–1010.

Simonini, P., and S. Cola, 2000, Use of piezocone to predict maximum stiffness of venetian soils: Journal of Geotechnical and Geoenvironmental Engineering, **126**, 4, 378-382, doi: 10.1061/(ASCE)1090-0241(2000)126:4(378).

Sully, J. P., and R. G. Campanella, 1995, Evaluation of in situ anisotropy from crosshole and downhole shear wave velocity measurements: Geotechnique, **45**, 2, 267–282, doi: 10.1680/geot.1995.45.2.267.

Zhubayev, A., and R. Ghose, 2011, Physics-based integration of shear-wave dispersion properties for soil property estimation: Laboratory investigation: 81st Annual International Meeting, SEG, Expanded Abstracts, 1343–1374.

Zhubayev, A., and R. Ghose, 2012, Contrasting behavior between dispersive seismic velocity and attenuation: Advantages in subsoil characterization: Journal of the Acoustical Society of America, **131**, 2, EL170–EL176, doi: 10.1121/1.3678692.

Downloaded 27 Apr 2012 to 131.180.60.197. Redistribution subject to SEG license or copyright; see Terms of Use at http://segdl.org/